Nonequilibrium Molecular Dynamics Calculation of the Thermal Conductivity of Solid Materials

Henry J. Castejon*

Science Computing, University of Notre Dame, Notre Dame, Indiana 46556

Received: May 13, 2002; In Final Form: September 3, 2002

Tully's stochastic classical trajectory method to simulate lattice dynamics has been adapted to carry out nonequilibrium molecular dynamics calculations. The method allows for a computational experiment to be performed placing the material between two heat reservoirs at different temperatures: the resulting temperature gradient generates thermal stationary nonequilibrium states in the system. A phenomenological calculation of the thermal conductivity of the material is carried out by using Fourier's law. When applied to crystalline silicon, the method accurately describes the variation of the thermal conductivity with temperature.

I. Introduction

Semiconductors and insulators lack conducting electrons. Therefore, their thermal transport properties are primarily determined by lattice dynamics. The heat transfer is thus significantly affected by phonon-scattering processes such as phonon-defect and phonon−phonon interactions. The phenomenological coefficients describing the heat transfer and many other transport properties can be expressed in terms of time-correlation functions by using the Kubo formalism.[1] The main advantage of this approach is the generality of the resulting formulas, which can then be applied in any density regime. A calculation of time-correlation functions, however, is not a trivial matter; they require simulation times several times longer than the characteristic relaxation time of the correlation itself, which makes them computationally expensive. Nonequilibrium molecular dynamics (NEMD) can alternatively be used to carry out a phenomenological description of the heat transport process in solid materials.[2,3] With this approach it is possible to create stationary nonequilibrium states using temperature gradients produced by placing the material between two heat reservoirs at different fixed temperatures. A computational experiment can then be performed to determine the thermal conductivity of the material. This method is computationally less intensive and more accurate than the linear response techniques, since it deals with the signal itself instead of its average fluctuations in the equilibrium state. The method also provides a direct connection between the lattice dynamics and the thermodynamic properties of the material. In this work, Tully's stochastic classical trajectory method[4] to simulate lattice dynamics is adapted to generate stationary nonequilibrium states in order to examine the properties of solid materials in a nonequilibrium thermal regime. This method is then used to perform a NEMD simulation of the heat transport in crystalline silicon. As part of a larger project, this work also explores the possibility of using such calculations as a parametrization mechanism to determine intramolecular potentials suitable for the calculation of properties of solid materials.

II. Computational Methodology

The computational experiment is carried out by adapting the stochastic classical trajectory method of Tully[4] to simulate a stationary temperature gradient. This method uses a combination of Brownian and molecular dynamics to generate systems at a constant temperature. Although the full derivation of the mathematical formalism has been given elsewhere,[5] for clarity, a brief description of the method is presented here. The system is divided into primary and secondary zones that interact with each other according to a particular potential function. The coordinates of the atoms in the primary zone evolve according to the classical equations of motion for a particle i of mass m in a potential V:

$$m_{i,\mathrm{p}}\ddot{\boldsymbol{r}}_{i,\mathrm{p}} = -\sum_{i\neq j}\frac{\partial V(r_{ij})}{\partial r_{ij}} \tag{1}$$

where the subscript "p" refers to atoms in the primary zone. The atoms in the secondary zone are treated with a set of modified equations that include two additional terms representing the effect of the infinite number of atoms in the bulk of the material:

$$m_{i,\mathrm{s}}\ddot{\boldsymbol{r}}_{i,\mathrm{s}} = -\sum_{i\neq j}\frac{\partial V(r_{ij})}{\partial r_{ij}} - m_{i,\mathrm{s}}\beta\dot{\boldsymbol{r}}_{i,\mathrm{s}} + \mathrm{R}_{i,\mathrm{s}} \tag{2}$$

where "s" refers to atoms in the secondary zone. β is a friction coefficient, and R_i is a random force with a white spectrum.[6] The first of these two terms is a generalized friction force. It accounts for the dissipation of energy from the secondary zone to the rest of the material. The second one is a fluctuating force that accounts for the transfer of heat, due to the thermal vibrations, from the bulk of the material to the secondary zone. These terms rigorously satisfy the fluctuation−dissipation theorem,[7] and they balance each other while maintaining the proper temperature in the secondary zone. The simulated system consists of a slab of 500 atoms of silicon with horizontal (i.e., $x-y$ directions) periodic boundary conditions. Two secondary zones with different temperatures, as shown in Figure 1, were placed at the top and at the bottom of the slab to represent the interaction of the atoms in the primary zone with two heat reservoirs at different temperatures. The atoms in the secondary zones are anchored to lattice sites with springs whose force constants were selected to reproduce the lattice dynamics of

* To whom correspondence should be addressed. E-mail: hcastejo@nd.edu.

10.1021/jp021189z CCC: $25.00
Published on Web 12/17/2002

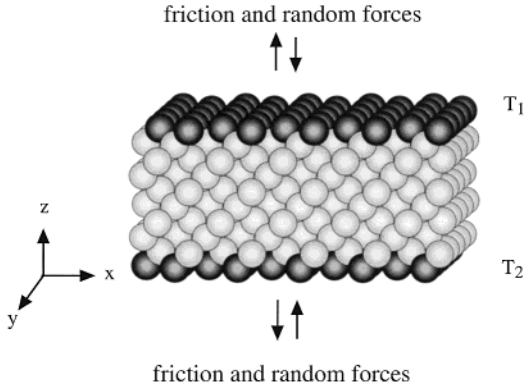

Figure 1. Illustration of a simulated system. Friction and random forces were applied to the top and bottom layers to keep their temperature constant.

the solid. They were subjected to random and friction forces which were generated in such a way as to rigorously satisfy the fluctuation−dissipation theorem and maintain their respective temperatures at a constant value. Thus, a thermal gradient was established along the *z*-direction of the slab. The top layer resides at the lower temperature and the bottom layer at the higher one. All atoms were assumed to interact via a pairwise additive Morse potential of the form

$$V(r) = \epsilon(1 - e^{-\alpha(r-r_o)})^2 \quad (3)$$

The values of the binding strength ($\epsilon = 78.50$ kJ/mol) and the energy transfer ($\alpha = 1.955$ Å^{-1}) parameters were selected to best reproduce the frequency cutoff of 16.0 THz in the phonon spectrum of Si.[8] The calculated value was 19.0 THz. No spectral details were sought since that would require a potential with three-body interaction terms.[9] The equilibrium distances r_o for each atomic pair were taken to be those in the crystalline solid. The structural integrity of the slab was verified after every calculation, and the potential was terminated at a distance equal to one-third of the slab's height (i.e., 3.90 Å). A Morse-type potential should suffice to describe the dynamics here, since no alterations of the lattice are taking place and therefore the atoms vibrate in a harmonic fashion.

III. Stationary Nonequilibrium States

The computational experiment begins with the realization of an equilibrium thermodynamic state at a given temperature by setting both secondary zones at the same temperature. The simulation is continued until a constant temperature state is reached for the whole slab. Then, the temperature of the secondary zone at the top of the slab is set down to a value lower than that at the bottom of the slab. After that, the system enters into a transient stage which relaxes to a stationary nonequilibrium state with a thermal gradient along the *z* direction. Relaxation times to reach a stationary temperature profile were in the order of 10 ps. Figure 2 shows the temperature profile when the two secondary zones are set at a temperature difference of 100 K. The temperature gradient was obtained by dividing the slab into multiple layers perpendicular to the *z*-axis and then calculating the temperature of each individual layer. The outermost layers at the top and at the bottom of the slab were not included in the calculation of the gradient. A temperature difference of 100 K is equivalent to imposing gradient of 8.2×10^8 K cm^{-1}, which is within the linear response range of Fourier's law. No systematic deviations from this law have been found for temperature gradients up to

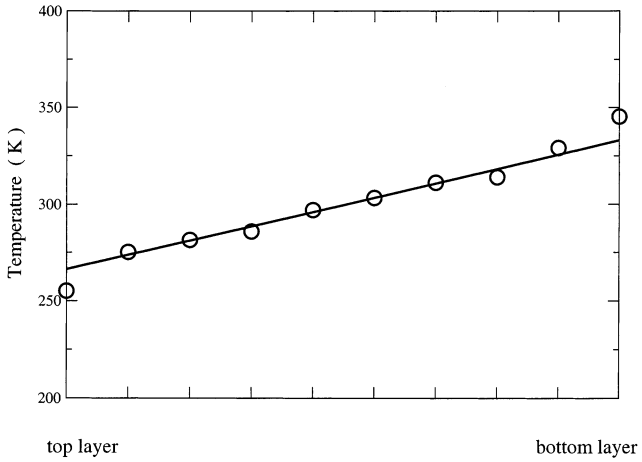

Figure 2. Temperature profile for a temperature difference of 100 K. Circles are the layer temperature. The solid line is the fitted profile using only the internal layers. The correlation coefficient is 0.992.

2.0×10^9 K cm^{-1}.[10] The thermalization mechanism, however, yields a thermal gradient that is lower than the applied one, but still fairly linear within the bulk of the material. This feature characterizes all simulations independent of the magnitude of the applied gradient and/or the length of the simulation. A lower temperature gradient appears to be, however, a parametrization penalty, since a higher one can be obtained by increasing the value of some of the potential parameters.

The calculated gradient was used to determine the thermodynamic properties, since it represents the response of the system to the imposed conditions. This is effectively equivalent to rescaling the parameters of the simulation. The properties of the outermost layers were not used to obtain the final results. Their temperatures were obtained by extrapolating the temperature profile in the bulk of the material. The uncertainty in the temperature of the layers was calculated from the statistical noise in the *xy* plane for each individual layer. It was found to be consistently between 10 and 15% of the temperature value for each respective layer. It should be noticed, however, that the uncertainty in the temperature is mainly statistical. This uncertainty could be lowered by increasing the number of particles per layer, i.e., by enlarging the system. This, however, will also increase the time needed for the system to relax completely. To ensure the linearity of the phenomenological laws no temperature difference greater than 150 K was imposed on the system. The temperature of the outermost layers was obtained by extrapolating the bulk temperature profile. For all of the studied gradients the extrapolated temperature differed from the calculated one, that difference was always smaller than the statistical uncertainty in the temperature. The efficiency of the thermalization mechanism makes it possible for the system to relax fully within a time period suitable for the realization of the computational experiment. It also permits the use of small imposed gradients (e.g., 50 K) relative to the size of the system, which increases the precision of the calculated heat currents. A temperature difference of 100 K was used to generate the temperature gradient in the final calculations. This value was almost 10 times larger than the statistical uncertainty in the temperature of each layer, and it was sufficiently small to ensure the linear behavior of the hydrodynamic equations. The final results of this was a linear temperature profile through the system that yielded thermal stationary states in which the time-averaged heat current was uniform within the statistical noise for all layers.

IV. Thermal Conductivity

If the macroscopic field gradients are not too large, the phenomenological laws remain linear, and the relations (e.g., Fourier's law) between thermodynamic forces and fluxes can be expressed using transport coefficients.[11] Since the system is in a stationary state, but not in equilibrium, the calculation of the thermodynamic properties is carried out using the local equilibrium hypothesis. Thus, the system is divided in pieces. Each piece is postulated to be at equilibrium. It can be assigned values of thermodynamic properties and all the usual relations between such variables hold. Here, the system was divided into layers parallel to the secondary zones and perpendicular to the temperature gradient. The heat current density can be calculated in terms of properties of each individual atom in the solid by using Kirkwood's equation[12] expressed in the center-of-mass reference frame:

$$\boldsymbol{q}_i(\boldsymbol{r};t) = \left[v_i \cdot E_i + \frac{1}{2}\sum_{i \neq j} \boldsymbol{r}_{ij} \cdot (\boldsymbol{F}_{ij} \cdot \boldsymbol{v}_i) \right] \delta(\boldsymbol{r}_i - \boldsymbol{r}) \qquad (4)$$

This formula was derived for a central force potential. Although some applications with a three body potential have been reported,[13] these require an arbitrary partitioning of the potential energy. The first term in the right-hand side represents the transport of kinetic energy by convection mechanisms and is a measure of the atomic diffusion. This term is not important in the case of a solid since the atoms vibrate in a harmonic fashion. It becomes appreciable only at high temperatures near melting. The second term is the contribution of the particle interaction to the heat transfer. This is the dominant component in solids. The time-averaged heat current in the k layer is

$$\boldsymbol{q}_k = \langle \boldsymbol{q}_i(r,t) \rangle \qquad (5)$$

where the brackets represent the canonical ensemble average. The thermal conductivity is finally obtained from the phenomenological description for heat transfer (i.e., Fourier's law):

$$\boldsymbol{q} = -k\nabla T \qquad (6)$$

The smoothed value for the heat flux across the slab is obtained by averaging over the internal layers. The temperature gradient is calculated as described in the previous section. The outermost layers have been excluded from the calculation, since any thermodynamic property will be affected by the altered force field due to the absence of particle images in one side along the z direction. This effect is diluted on going into the bulk. Along the x and y directions, periodic boundary conditions provide the correct representation of the simulation domain for energy transport.[14] The results are shown in Figure 3 along with the experimental values[15] and data obtained using linear response theory (LRT).[14] Although the method underestimates the thermal conductivity of Si, the calculated values are of the same order of magnitude as the experimental and LRT data. The method also describes the expected trend correctly. That is, the thermal conductivity decreases with increasing temperature. This is due mainly to anharmonic effects that become predominant at high temperatures.

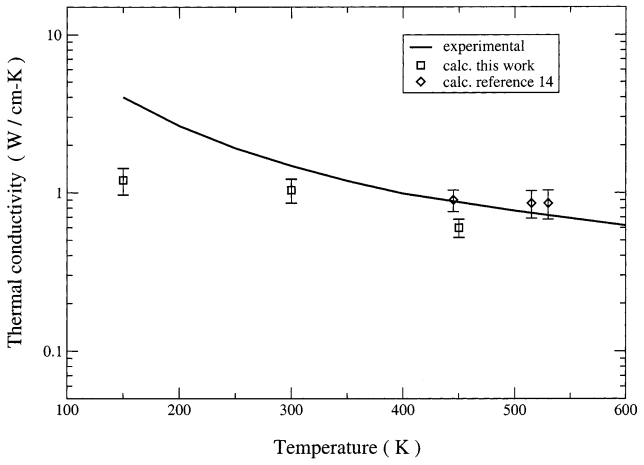

Figure 3. Thermal conductivity vs temperature for crystalline silicon.

V. Conclusions

The generalized Langevin based technique presented here can yield stationary nonequilibrium thermodynamic states in a canonical molecular dynamics system. Relaxation times found in such a system are sufficiently short to allow for a computational experiment to be carried out to study thermodynamic properties of solid materials in non equilibrium thermal regimes. The thermal exchange, provided by the stochastic layers of the simulated system, is sufficiently efficient to allow for the simulation of lower gradients than those previously reported. This ensures the validity of the phenomenological laws (e.g., Fourier's law). The linearity of the temperature gradients obtained indicates that the local equilibrium hypothesis holds for the bulk of the material. This makes a description of the heat transport in that region possible. This technique also provides a suitable method to parametrize the interaction potentials in solid phases using a measurable thermodynamic property. We also note that the effect on the thermodynamic properties of having a direction with nonperiodic boundary conditions could be minimized by extending the system along that particular direction.

References and Notes

(1) McQuarrie, D. A. *Statistical Mechanics*; Harper and Row: New York, 1976.
(2) Hoover, W. G. *Annu. Rev. Phys. Chem.* **1983**, *34*, 103−127.
(3) Haile, J. M. *Molecular Dynamics Simulation: Elementary Methods*; John Wiley & Sons: New York, 1992.
(4) Tully, J. C. *Acc. Chem. Res.* **1981**, *14*, 188. Tully, J. C. In *Many Body Phenomena at Surfaces*; Langreth, D., Suhl, H., Eds.; Academic: New York, 1984; pp 377−401.
(5) Tully, J. C. *J. Chem. Phys.* **1980**, *73*, 1975.
(6) Hansen, J. P.; McDonald, I. R. *Theory of Simple Liquids*; Academic Press: San Diego, 1986; pp 206−208.
(7) Kubo, R. *Rep. Prog. Theor. Phys.* **1966**, *29*, 255.
(8) Flensburg, C.; Stewart, R. F. *Phys. Rev. B.* **1999**, *60*, 284.
(9) Kittel, C. *Introduction to Solid State Physics*, 7th ed.; John Wiley: New York, 1996.
(10) Tenebaum, A.; Ciccotti, G.; Gallico, R. *Phys. Rev. A.* **1982**, *25*, 2778.
(11) Kirkaldy, J. S.; Young, D. J. *Diffusion in the Condensed State*; Institute of Metals, North American Publications Center: Brookfield, VT, 1987; p 137.
(12) Irving, J. H.; Kirkwood, J. G. *J. Chem. Phys.* **1950**, *18*, 817.
(13) Lee, Y. H.; Biswas, R.; Soukoulis, C. M.; Wang, C. Z.; Chan, C. T.; Ho, K. M. *Phys. Rev. B.* **1991**, *43*, 6573.
(14) Volz, S.; Chen, G. *Phys. B* **1991**, *263*−*264*, 709−712.
(15) Lide, D. R. *Handbook of Chemistry and Physics*, 82nd ed.; CRC Press: New York, 2001; pp 12−222.